CCB-based encapsulation of pyrite for remediation of acid mine drainage

Sowmya Bulusu [a], Ahmet H. Aydilek [b,*], Neha Rustagi [c]

[a] *Geosyntec Consultants, Inc., 1255 Roberts Boulevard NW, Suite 200, Kennesaw, GA 30144, USA*
[b] *Department of Civil and Environmental Engineering, University of Maryland, 1163 Glenn Martin Hall, College Park, MD 20742, USA*
[c] *Department of Civil and Environmental Engineeringg, University of Maryland, 1173 Glenn Martin Hall, College Park, MD 20742, USA*

Abstract

Acid mine drainage (AMD) from abandoned coal mines continues to be one of the most significant environmental problems. Remediation of AMD requires an addition of lime source to decrease the acidity, and grouting the entire mine and encapsulating the pyrite by calcium-rich additives is often employed. Utilization of alkaline coal combustion by-products (CCBs) has gained acceptance in such remediation applications because of their cost-effectiveness. A study was conducted to investigate the effectiveness of CCBs to abate acid mine drainage by encapsulation of pyrite. Geomechanical, hydraulic, and environmental tests were performed on grouts prepared with various ratios of CCBs as well as an alternative free lime source, lime kiln dust (LKD). The results indicated that the mechanical properties of grouts were dependent on their free lime contents. Hydraulic conductivities of pyrite–grout columns were relatively high due to the coating of the pyrite rock with the grout rather than the filling of all of the void spaces, as commonly experienced in field applications. The leaching tests indicated that the presence of high amounts of lime in a grout is not solely sufficient to improve the quality of AMD, since the rate of dissolution of a high lime content grout may be slow due to its rapid hardening. Therefore, it is recommended that grouts be selected with consideration of their hardening capacities, as well as the percentage of lime content present in the mixture.
© 2007 Elsevier B.V. All rights reserved.

Keywords: Coal combustion by-product; Acid mine drainage; Encapsulation; Neutralization; Pyrite oxidation

1. Introduction

Acid mine drainage (AMD) is commonly encountered in the vicinity of abandoned coal mines. It is formed due to the oxidation of sulfur bearing minerals such as pyrite that is abundantly present in and around coal seams. Iron hydroxide, iron sulfate, and sulfuric acid are formed as a result of a series of geochemical and microbial reactions on the pyrite. Thus, highly acidic water that contains large amounts of dissolved metals is discharged into the environment and causes severe damage to all forms of life.

In the last few decades, many in situ abiotic and biological treatment technologies have been developed to remediate abandoned mines producing AMD. The application of alkaline products directly into the mine discharge [1–3] or incorporation of them into soil via trenches or as mine overburden [4–10] is a popular remediation technique. However, these high-cost techniques pose various problems due to the formation of metal precipitates and the armoring of the alkaline products [6,11,12].

Injection of lime-rich grout into abandoned underground coal mines is a popular technique that provides a permanent solution to control AMD [13–16]. The injected grout penetrates into the pyritic rock present on the mine pavement and shaft, entombs the pyrite, and forms a long-term barrier between the pyrite and water and oxygen. This sequence reduces the potential for acid formation. Among various lime sources, coal combustion by-products (CCBs) provide a cost effective solution. Some of the CCBs, such as flue gas desulfurization (FGD) and fluidized bed combustion (FBC) by-products are highly alkaline in nature due to the presence of unreacted lime (calcium oxide). Alkaline CCBs or other additives rich in free lime (CaO) can be mixed with Class F fly ash and water to prepare a grout that upon curing hardens like cement. Such grouts typically have relatively lower hydraulic conductivity as compared to the mine walls, which is necessary to fill mine voids and limit the mine from any contact with water or oxygen in a field remediation application [13,17]. In addition to mine sealing, these alkaline CCB-based grouts also neutralize the AMD that is formed at the source, providing an integrated solution to the remediation of abandoned mines.

In spite of the fact that extensive research and field applications have been conducted for CCB grouting of underground mines, the emphasis is usually on filling all of the mine voids with low permeability grout. However, as reported by Taerakul et al. [16] as well as through the observations made in a recent project conducted by Bulusu et al. [18] in Western Maryland, the total filling of a mine is not possible in most cases due to unknown voids that exist or the limited penetration of the grout into deep mine voids and pyritic rock on the mine pavement. Thus, it is more practical to aim at proper "encapsulation" of the pyritic rock in the mine pavements and shafts than to expect an entire filling of mine voids.

The objectives of the current study were to determine if CCBs have suitable geotechnical and environmental properties for use in remediation of abandoned coal mines and to study how the encapsulation of acid-leaching pyrite occurs with the CCBs. To meet these objectives, a series of geomechanical and environmental laboratory tests were conducted on various grouts prepared with different proportions of CCBs that were collected from Maryland power plants. Additionally, lime kiln dust (LKD) was used in some mixtures as an alternative alkalinity source. Spread, slump, bleed, and unconfined compressive strength tests were performed in order to arrive at optimal grout mixtures. These mixtures were then evaluated for their potential to encapsulate the pyrite rock in mine pavements and shafts through a series of hydraulic conductivity and column leaching tests.

2. Materials

A mixture of Class F fly ash and bottom ash (FA–BA), FBC by-product, lime kiln dust, pyrite, and College Park tap water were used to prepare the grouts. The FA–BA material was obtained from the R. Paul Smith Power Plant in Williamsport, Maryland. This fly ash–bottom ash mixture was placed outside the power plant in large heaps. Thus, the material had to be sieved through U.S. No. 8 (2.36 mm) and No. 16 (1.18 mm) sieves to remove any local shale and weeds present. Atterberg limit tests conducted on the ash mixture per ASTM D 4318 indicated that the material was non-plastic. The non-plastic fluidized bed combustion (FBC) by-product was obtained from the Warrior Run Power Plant in Cumberland, Maryland. The lime kiln dust (LKD) was obtained from Carmeuse Natural Chemicals Company located in Pittsburgh, Pennsylvania. This material was also non-plastic. The iron pyrite used in this study was collected from the Kempton Mine Complex located in Kempton, Maryland. It had a specific gravity of 4.9 and was classified as well-graded gravel (GW) according to the Unified Soil Classification System (USCS). The physiochemical properties of the FA–BA mixture, FBC by-product, lime kiln dust, and pyrite are shown in Table 1.

3. Methods

3.1. Laboratory evaluation of geomechanical properties

The grout mixtures were prepared with different proportions of the base material (FA–BA mix), lime activator (FBC

Table 1
Physical and chemical properties of the materials used in the study

Property	FA–BA	FBC	LKD	Pyrite
Physical properties				
D_{10} (mm)	0.003	0.002	0.009	7
D_{30} (mm)	0.011	0.003	0.011	10.2
D_{85} (mm)	0.15	0.004	0.02	11.1
C_u	9.33	1.5	1.44	1.5
C_c	1.44	1.5	1.03	1.4
Fines content (%)	75.6	88.7	89.9	–
Moisture content (%)	21.8	0	0	–
Chemical	**FA–BA**	**FBC**	**LKD**	**Pyrite**
Chemical constituents				
SiO_2 (%)	48.8	32.8	4	–
Al_2O_3 (%)	24.5	15.1	2.4	–
CaO (%)	0.94	14.7	60.7	–
Fe_2O_3 (%)	9.1	5.5	0.69	–
Cr_2O_3 (%)	0.03	0.01	<0.01	–
K_2O (%)	2.1	1.7	0.8	–
MgO (%)	0.62	2.3	2.1	–
MnO (%)	0.02	0.02	<0.01	–
Na_2O (%)	0.3	0.2	0.09	–
P_2O_5 (%)	0.3	0.6	0.02	–
TiO_2 (%)	1.3	0.74	0.1	–
BaO (%)	0.1	0.1	0.01	–
SrO (%)	0.06	0.12	0.02	–
LOI (%)	11.8	21.1	27.8	–
Trace elements	–	5.01	1.27	–
Total Fe (%)	–	–	–	45.9
Total S (%)	–	–	–	54.1

Note: FA: fly ash; BA: bottom ash; FBC: fluidized bed combustion ash; LKD: lime kiln dust; LOI: loss on ignition (=total carbon).

by-product or LKD), and water. Therefore, the mixtures were classified as FBC-based and LKD-based mixtures. The mixtures encompassed a range of base and activator percentages to observe their effect on various geotechnical properties. Grouts with very high percentages of activator (>70%) were not considered during testing, since mixing and handling of grout was very difficult and the grout hardened very quickly.

A total of 45 different grout mixtures, 22 mixtures with FBC by-product and 23 with LKD, were prepared (Tables 2a and 2b). The water contents of the grouts were varied within each mixture to obtain the "optimal" water content that provided good grout flowability. Good flowability was defined as a horizontal spread value of at least 200 mm and a slump of between 200 and 250 mm. However, considering the reported difficulties encountered with interpretation of slump tests [19], spread tests (ASTM D6103) were chosen to delineate the "optimal" water contents. Fourteen of the initial 45 mixtures that resulted in a spread of 200 mm or higher were selected (mixtures shown in bold in Tables 2a and 2b). These 14 grout mixtures were then tested for slump (ASTM C 143/C 143 M) at their corresponding "optimal" water contents. Bleed of the freshly prepared grout was measured for these 14 mixtures using the procedures outlined in ASTM C 940. Unconfined compressive strength tests were conducted on cylindrical grout specimens 102 mm in diameter and 203 mm in height after curing them for 7, 14, and 28 days.

Table 2a
Mixture proportions and initial testing of FBC-based grout mixtures

Specimen ID	FA–BA (%)	FBC (%)	Water content (%)	Spread (mm)
F1 (a)	30	70	35	NA
F1 (b)	30	70	50	NA
F1 (c)	30	70	80	105
F1 (d)	30	70	88	130
F1 (e)	30	70	92	190
F1 (f)	**30**	**70**	**93**	**205**
F2 (a)	40	60	80	120
F2 (b)	40	60	83	150
F2 (c)	40	60	85	185
F2 (d)	**40**	**60**	**88**	**210**
F3 (a)	50	50	75	165
F3 (b)	50	50	78	165
F3 (c)	**50**	**50**	**80**	**210**
F4 (a)	60	40	70	195
F4 (b)	**60**	**40**	**71**	**210**
F5 (a)	70	30	60	145
F5 (b)	**70**	**30**	**63**	**200**
F5 (c)	70	30	65	225
F6 (a)	80	20	55	175
F6 (b)	**80**	**20**	**58**	**210**
F7 (a)	90	10	44	278
F7 (b)	**90**	**10**	**40**	**204**

Note: All percentages are by weight. NA: not applicable due to insufficient amount of water content for preparation of a homogeneous grout mixture. The mixtures in bold resulted in a spread of 200 mm or higher.

For two of the mixes that had low 14-day compressive strengths (F3 and F4), the strength was determined after curing for 56 days instead of 28 days. Most mixing was done by hand as recommended in ASTM C 192/C 192M. For slump measurements,

Table 2b
Mixture proportions and initial testing of LKD-based grout mixtures

Specimen ID	FA–BA (%)	LKD (%)	Water content (%)	Spread (mm)
L1 (a)	30	70	45	155
L1 (b)	30	70	53	290
L1 (c)	30	70	52	275
L1 (d)	30	70	51	234
L1 (e)	**30**	**70**	**50**	**200**
L2 (a)	40	60	50	170
L2 (b)	**40**	**60**	**52**	**204**
L3 (a)	50	50	55	270
L3 (b)	50	50	40	95
L3 (c)	50	50	45	120
L3 (d)	50	50	48	178
L3 (e)	**50**	**50**	**50**	**210**
L4 (a)	60	40	40	Failed
L4 (b)	60	40	45	154
L4 (c)	**60**	**40**	**48**	**205**
L5 (a)	70	30	40	162
L5 (a)	70	30	45	225
L5 (c)	**70**	**30**	**44**	**202**
L6 (a)	80	20	35	Failed
L6 (b)	80	20	40	153
L6 (c)	**80**	**20**	**42**	**203**
L7 (a)	90	10	33	185
L7 (b)	**90**	**10**	**35**	**210**

Note: All percentages are by weight. Failed: the specimen did not have any spread due to shear failure. The mixtures in bold resulted in a spread of 200 mm or higher.

a large concrete mixer was used to mix the large quantities of grout required.

3.2. Laboratory evaluation of hydraulic conductivity and leaching behavior

Pyrite exists on the pavements or on the walls of shafts of abandoned mines, as illustrated in Fig. 1. Rainwater and/or groundwater (depending on the elevation of mine pavement with respect to groundwater table) along with oxygen may interact with the pyrite and result in the formation of AMD. As seen from Fig. 1, the injected grout may not penetrate into deeper voids of the pyrite, but instead would form a barrier between the pyrite and the environment, rather than closing (filling) of the mine voids [20].

It has been inferred from the two recent studies that the total filling of a mine with grout is usually not possible because all voids will not be penetrated by the grout in the mine pavement [16,18]. This was evident from the flow rates that were not altered greatly at both mine sites even after the grouting operation was completed. However, significant but slow improvement in the quality of water discharged from the mines was observed. Therefore, it seems reasonable to conclude that the goal should be sufficient "encapsulation" of the pyritic rock in the mine pavements and shafts rather than the entire filling of mine voids for an AMD remediation application.

In order to evaluate the hydraulic performance and leaching behavior of grout-encapsulated pyrite, long-term laboratory flow tests were conducted. Eight of the 14 grouts, F2 through F6 and L3 through L5, were mixed with pyrite following the procedures described in ASTM C 192/C 192 M and placed in clear PVC columns 100 mm in diameter and 200 mm in height. Preliminary analyses were made to calculate the amount of grout that would be needed to fill nearly all of the voids inside the pyrite rock that had a porosity of 0.32. The debris and large size particles in the pyrite rock were pulverized until they passed through a 38.1-mm sieve. Additionally, small size particles in the rock were eliminated by sieving through a 2.36-mm sieve (U.S. sieve size No. 8). A photograph of the grout-encapsulated pyrite column is shown in Fig. 2.

The hydraulic conductivity of each pyrite–grout mixture was determined using the constant head method in accordance with ASTM D 5856. The specimens were cured for 7 days at 100% relative humidity and at $21 \pm 2\,^{\circ}C$ for equilibrium inside the rigid-wall PVC cells before initiating the tests. The only exception was F6, which was cured for 14 days since the grout did not set within 7 days. The influent was College Park water, which had a pH of 7.8, comparable with the properties of water in the natural environment [21,22]. The flow was maintained from top to bottom and a hydraulic gradient of 2.5 was selected based on the effective stress conditions present in mine pavements. Each test was terminated after a steady-state rate of flow was achieved which met the criteria of ASTM D 5856. The termination criteria were satisfied when four consecutive values of the steady-state curve varied within the 25% of their mean value and when the Q_{out}/Q_{in} was between 0.75 and 1.25.
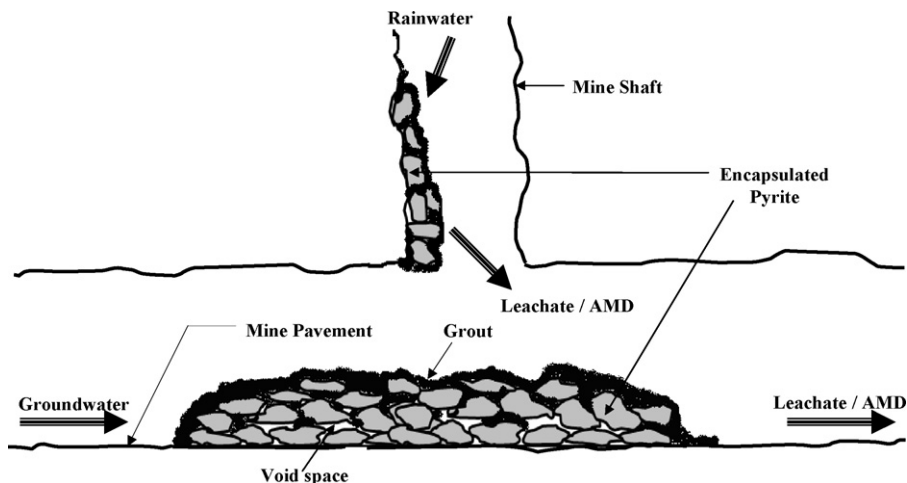
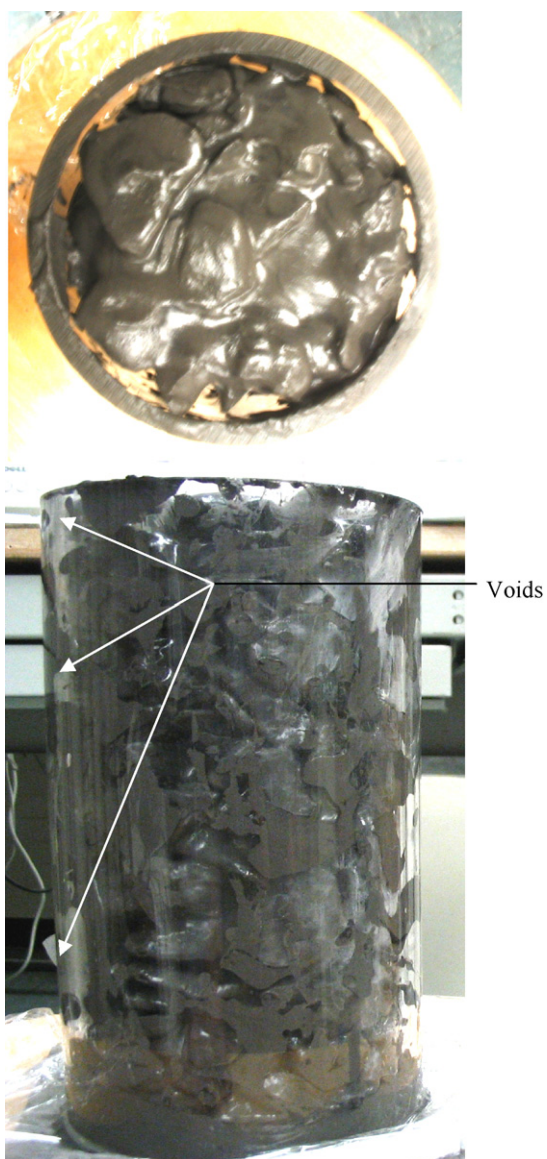Fig. 1. Grout-encapsulated pyrite in the mine pavement and shaft.

Fig. 2. Pyrite–grout column top and front views.

The leachate from effluent port was collected in 50-mL centrifuge tubes with caps and stored in the refrigerator at a temperature of 4 °C. Samples used for determination of metal concentrations were digested using concentrated nitric acid (HNO_3) to a pH < 2. Metal digestion with nitric acid is usually performed to reduce interference by organic matter and to convert the metals to a free form that can then be analyzed by atomic absorption spectrometry. After digestion, the samples were filtered using a Supor® 0.2 μm membrane filter. The samples analyzed for sulfate concentrations did not require digestion and were only filtered before the analysis. For quality assurance/quality control purposes, a blank was analyzed for every five samples to verify baseline stability for metal analyses conducted by atomic absorption spectrometer and for sulfate measurements conducted by ion chromatograph. A standard solution was also analyzed for every 10 samples to confirm the accuracy of the test results.

The pH of collected leachate samples was measured using an electrode pH meter (Mettler Toledo MA235 pH/Ion Analyzer). Two replicate pH readings were taken for each sample and the average value was reported as the pH of the sample. The concentrations of the iron and calcium in the leachate were measured by the direct air–acetylene flame method of atomic absorption spectrometry using a Perkin-Elmer AA 5100 spectrometer. Four standard concentrations were prepared and used for the calibration of the instrument to obtain a minimum coefficient of determination of 0.99 (i.e., $R^2 = 0.99$). The instrument reports the concentration of iron in a sample as the average of two measurements. The tests yielded a standard deviation of less than 1. Aluminum in the leachate samples was measured using an electrothermal atomic absorption spectrometer by Green Mountain Laboratories based in Vermont. The sulfate concentrations in the leachate were determined by using a Dionex DX-100 ion chromatograph. The flow rate of the carbonate–bicarbonate buffer (eluent) was maintained at 1 mL/min during operation of the chromatograph. Calibration curves were constructed with at least three standards prepared in the range of expected concentrations.

4. Results and discussion

4.1. Geomechanical properties

The spread of the 14 selected grout mixtures prepared at their "optimal" water contents are plotted versus FA–BA and free lime content/FA–BA ratio in Fig. 3. The effects of the same parameters on slump are shown in Fig. 4. The spread and slump cannot be directly included in the graphs, as each grout mixture involved different water content. Thus, the spread and slump of each specimen were normalized by their corresponding "optimal" water contents, which provided a ratio that is independent of the water content of the grout mixture.

The spread and slump decrease with increasing free lime content/FA–BA ratio for both FBC-based and LKD-based mixtures. This decrease can be attributed to pozzolanic hydration reactions that took place in the grout. Excess free lime consumes the water for hydration reactions and decreases the flowability of a grout. The rate of decrease is higher at relatively lower free lime content/FA–BA ratios, and the curve flattens at higher ratios. At higher FBC by-product or LKD contents (higher free lime content/FA–BA mix ratios), greater hydration took place in the grout. The flattening of the curve is likely due to the fact that the corresponding FA–BA contents are low at high FBC or LKD contents. The base material was not sufficient to react with the large amounts of available lime; therefore, the pozzolanic hydra-
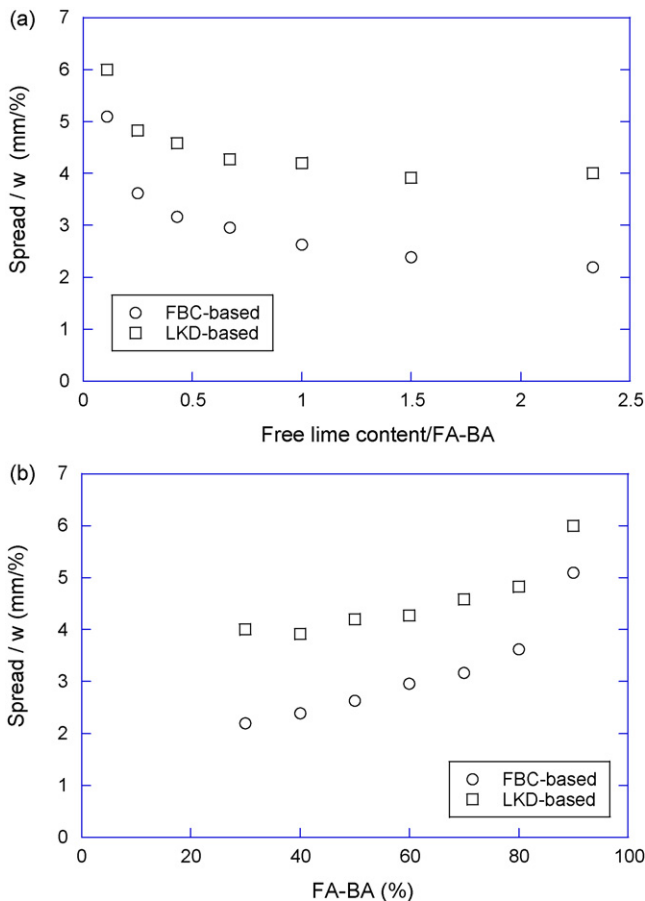
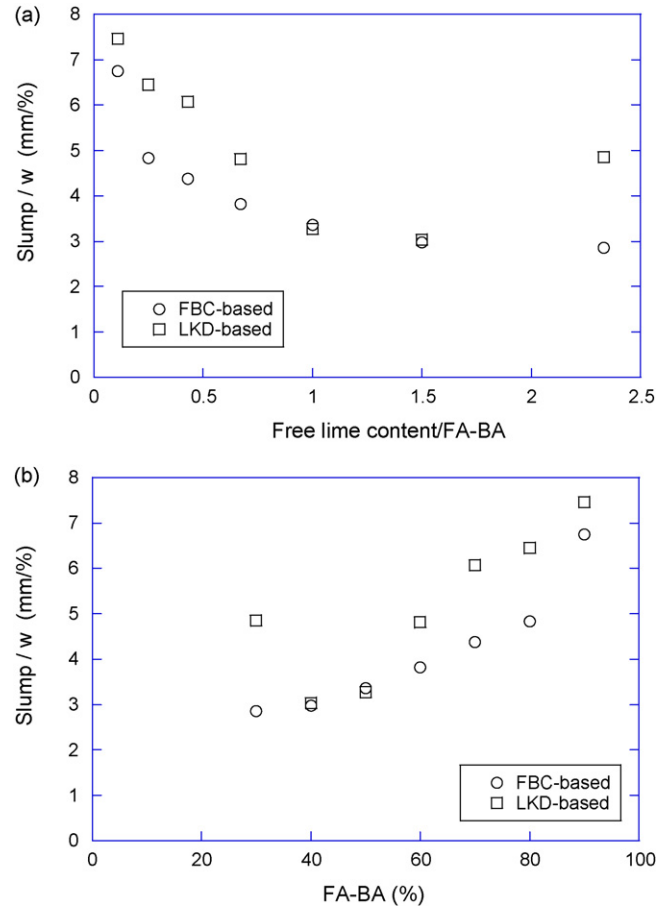Fig. 3. Spread/water content vs. (a) free lime content/FA–BA and (b) FA–BA%.

Fig. 4. Slump/water content vs. (a) free lime content/FA–BA and (b) FA–BA%.

tion reactions slowed down. On the other hand, the spread and slump demonstrate an increasing trend with increasing FA–BA contents for both types of grout mixtures, since the bulky base material aids in making the grout more flowable.

As the lime content of a grout mixture increases, more hydration reaction takes place, which uses larger amounts of water contained in the mix. Thus, the bleed decreases with an increasing free lime content/FA–BA ratio, as seen in Fig. 5a. Conversely, an increase in the quantity of FA–BA base material increases the bleed water mainly due to its granular structure (Fig. 5b) and, as a result, less hydration takes place. LKD-based mixtures L1 and L2 did not yield visible bleed water, therefore their bleed values were reported as zero. At a given free lime content/FA–BA ratio or FA–BA percentage, the FBC-based mixtures generally indicated higher bleed values when compared to the LKD-based mixtures. This may be attributed to the lower CaO content of the FBC by-product compared to that of LKD (14.7% versus 60.7%), which requires less water for hydration reactions to take place, and results in higher amounts of bleed water (i.e., excess water).

Unconfined compressive strengths of the mixtures are plotted against curing time in Fig. 6. Relatively high FA–BA content mixtures (F3, L3, F4, L4) have relatively low 7-day strengths; however, they gain strength after 14 days of curing. Fly ashes generally have a slow reactive nature but they gain substantial
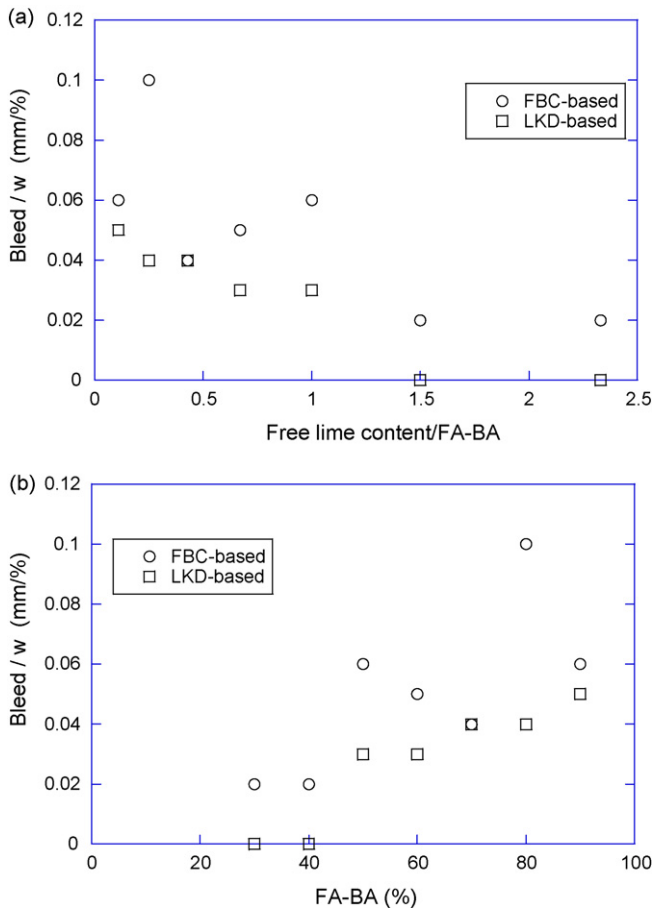
Fig. 5. Bleed/water content vs. (a) free lime content/FA–BA and (b) FA–BA%.

Fig. 6. Strength vs. curing time for (a) FBC-based and (b) LKD-based mixtures.

strength upon sufficient curing [23]. It is observed that the rate of strength gain is relatively low after 14 days for FBC-based specimens, compared to their 7-day strengths. This may be due to the relatively lower CaO content of FBC as compared to LKD. For LKD-based specimens prepared at high lime contents (i.e., all but L6 and L7), the 7-day strengths are relatively low and an appreciable strength gain is visible beyond 14 days.

4.2. Hydraulic conductivity

After the evaluation of geomechanical properties, eight grouts, F2 through F6 and L3 through L5, were selected based on their good flowability and relatively high strengths. These eight grout mixtures were then injected into the pore structure of the pyrite to simulate the pyrite–grout mixtures that would be present in mine pavements and on the walls of the mine shafts. All eight mixtures with the exception of L3 had spread and slump above 200 mm, which indicated good flowability. Furthermore, mixture F6 was selected to observe the behavior of a low free lime content grout in remediating AMD, even though it had a relatively low 28-day strength.

The measured hydraulic conductivities ranged from 5.3×10^{-5} to 2×10^{-2} and from 2.4×10^{-5} to 1.5×10^{-2} cm/s for the FBC-based and LKD-based pyrite grout mixtures, respectively. These hydraulic conductivities were higher than expected,
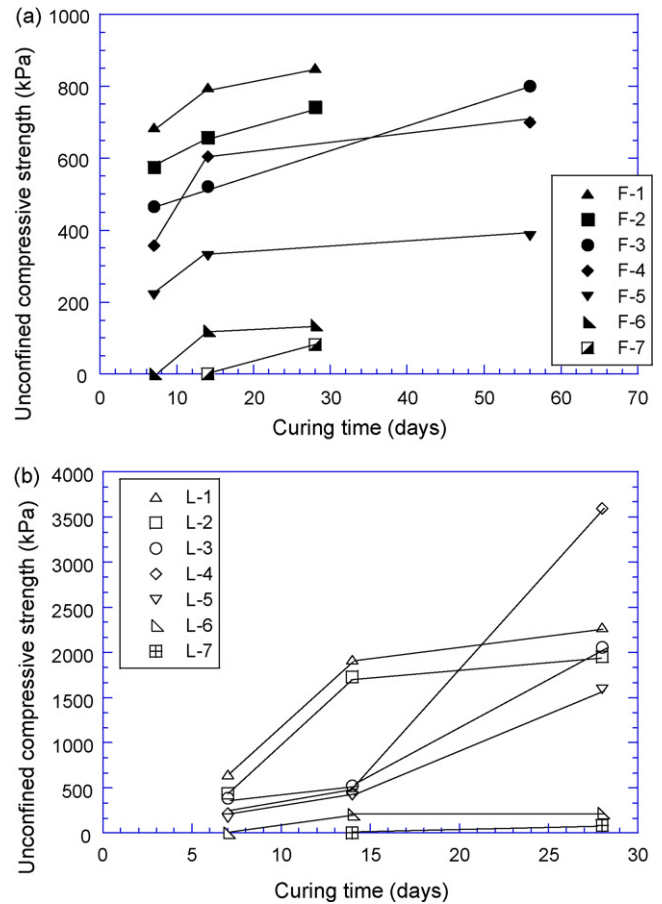
even though the volume of grout was nearly equal to the volume of voids present in the pyrite. This was attributed to the grout coating over the pyrite rock rather than the void spaces being filled, as commonly experienced in field applications. Similar observations were made by Bulusu et al. [18] in which the injection process required about $4300 \, m^3$ of grout although the volume of voids in the mine was initially estimated to be $3000 \, m^3$. Another reason may be the existence of a large unfilled void, which may have ultimately dominated the hydraulic conductivity.

The hydraulic conductivity is plotted against the free lime content/FA–BA ratio and the FA–BA content in Fig. 7. It is evident from Fig. 7 that the hydraulic conductivities decrease with increasing lime/FA–BA ratio. This may be attributed to a decrease in pore spaces at higher lime contents that resulted in a relatively lower amount of permeable grout in the column. The low hydraulic conductivities may also have been due to an increase in fines content associated with the presence of lime in the pyrite-grout column. Similar trends in permeability were observed by Gabr et al. [17] when fly ash was mixed with FBC and quicklime. In their study, hydraulic conductivities were reported to decrease by 0.5–3 orders of magnitude with a 5–15% increase in FBC content. Moreover, the hydraulic conductivities increase with increasing FA–BA contents mainly due to the coarse nature of the base material.
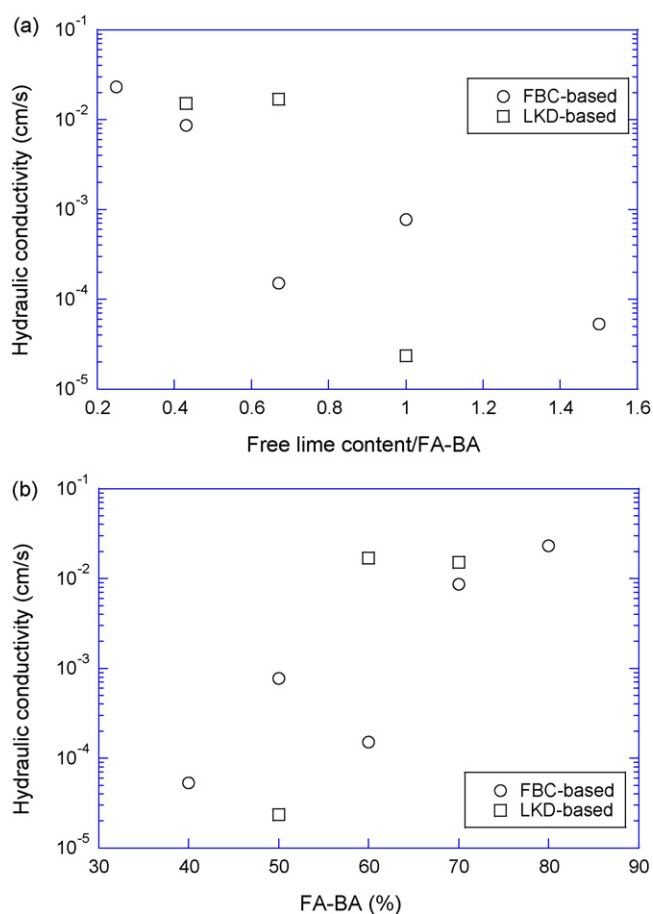
Fig. 7. Hydraulic conductivity vs. (a) free lime content/FA–BA, and (b) FA–BA%.

4.3. Leaching behavior

4.3.1. pH

The pH of leachate ranges from 7.6 to 8.5 for the FBC-based columns and from 8.8 to 12.3 for LKD-based columns, as shown in Fig. 8. The higher CaO content of LKD as compared to FBC results in higher pH values indicating dissolution of grout. The pH values are, in general, above the recommended range of pH
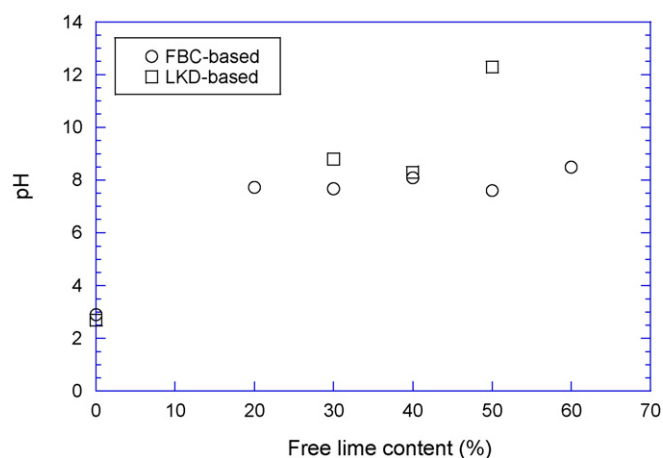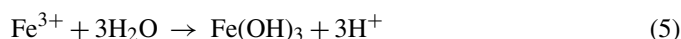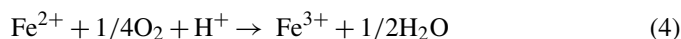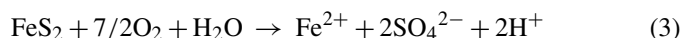

Fig. 8. Average pH vs. free lime content.

[24]. However, it should be noted that the U.S. EPA recommends secondary standards to water systems but does not require systems to comply; the limits are set only for aesthetic reasons, such as odor, taste, and color. The pH of AMD from the Kempton mine complex in western Maryland was measured to be 2.9, comparable with the pH of AMD reported in previous studies [25].
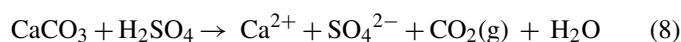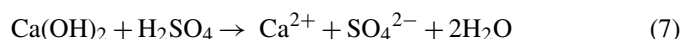
Fig. 8 suggests that the pH of leachate increases with increasing lime content due to the dissolution of the lime in the grout and possibly the neutralization of any acidity produced in the column. Alkalinity is produced due to reactions of CaO that is present in FBC and LKD with carbon dioxide (CO_2) and water in the environment. Calcium carbonate and calcium hydroxide are formed as a result of these reactions:

$$CaO + CO_2 \rightarrow CaCO_3 \tag{1}$$

$$CaO + H_2O \rightarrow Ca(OH)_2 \tag{2}$$

These two compounds not only contribute to an increase in pH directly, but also neutralize any acidity formed due to pyrite oxidation reactions. The chemical reactions that cause the oxidation of pyrite to form acidic water are as follows [26]:

$$FeS_2 + 7/2O_2 + H_2O \rightarrow Fe^{2+} + 2SO_4^{2-} + 2H^+ \tag{3}$$

$$Fe^{2+} + 1/4O_2 + H^+ \rightarrow Fe^{3+} + 1/2H_2O \tag{4}$$

$$Fe^{3+} + 3H_2O \rightarrow Fe(OH)_3 + 3H^+ \tag{5}$$

$$FeS_2 + 14Fe^{3+} + 8H_2O \rightarrow 15Fe^{2+} + 2SO_4^{2-} + 16H^+ \tag{6}$$

Neutralization reactions between the alkaline compounds and sulfuric acid formed due to pyrite oxidation reactions are as follows:

$$Ca(OH)_2 + H_2SO_4 \rightarrow Ca^{2+} + SO_4^{2-} + 2H_2O \tag{7}$$

$$CaCO_3 + H_2SO_4 \rightarrow Ca^{2+} + SO_4^{2-} + CO_2(g) + H_2O \tag{8}$$

The high pH due to the dissolution and neutralization reactions causes the dissolved metals in AMD to precipitate as hydroxides, thus remediating AMD. From the above neutralization reactions, it is possible to calculate the amount of carbonate/hydroxide alkalinity that needs to be applied in the field for a given acidity. However, it is generally difficult to quantify the amount of alkaline materials that need to be injected into a mine since fly ash–lime hydration reactions also consume some part of the alkalinity.

4.3.2. Iron

As observed from the pyrite oxidation chemistry defined in Eqs. (1) through (8), AMD consists of high levels of iron mainly in the soluble ferrous (Fe^{2+}) ion form. Iron is a major AMD-related parameter [25] and the U.S. EPA Water Quality Criteria (WQC) limit for iron in natural aquatic waters is 1 mg/L [24]. The temporal variations of Fe^{2+} concentration in the leachate collected from the FBC-based and LKD-based columns are shown in Fig. 9. The concentrations seem to follow a decreasing trend with time for FBC-based columns. The grout formed a barrier between the pyrite and water, which limited the oxidation of pyrite and formation of ferrous-rich acidic water. The high pH
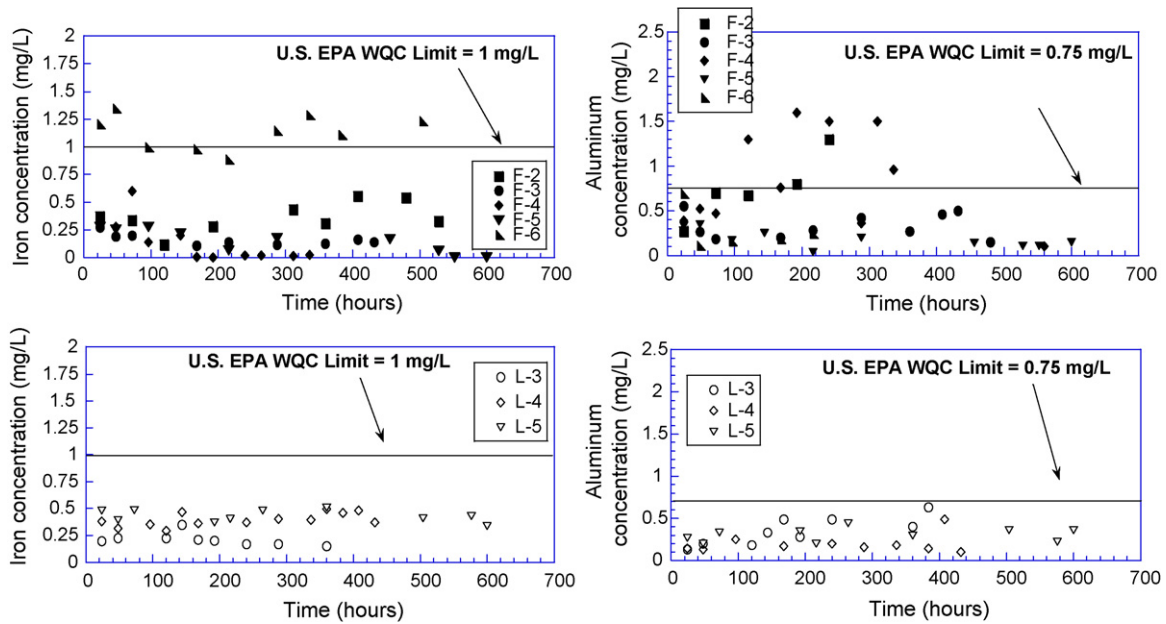
Fig. 9. Concentration of iron and aluminum in the effluent vs. time for FBC-based, and LKD-based grout mixtures.

due to dissolution of grout caused any ferrous iron to precipitate as an insoluble ferric hydroxide ($Fe(OH)_3$) into the leachate.

In general, iron concentrations stay in a constant but relatively higher range for LKD-based columns as compared to FBC-based columns, except F6. This may be due to two reasons. First, the LKD, which has higher CaO content than FBC, hardens faster and as a result dissolves at lower rates. As evidenced from the high pH values in Fig. 8, there is some dissolution of the LKD-grout, but this dissolution may not be at a rate that is required to cause a significant decrease in iron concentrations. Second, F6 included significant amounts of coarse-grained base materials (FA–BA) that resulted in a relatively high hydraulic conductivity. Such a porous nature of F6 may have caused leaching out excessive amounts of iron into the environment.

The effect of hardening of high-lime content grouts on iron concentrations can also be observed from Fig. 10. The average concentration of iron in the leachate follows an inverted bell-shaped trend with increasing free lime content/FA–BA ratio for FBC-based columns. The high iron concentrations observed at the low FBC/FA–BA ratio (0.25) may be due to the lower amount of free lime in the grout mixture that provides less alkalinity to precipitate iron. For a FBC/FA–BA ratio of above 1.0, iron concentrations increase because the dissolution rate is low due to rapid hardening of the grouts at high FBC contents (>50%). Similarly, the iron concentrations tend to increase at high LKD/FA–BA ratios; however, a conclusive statement cannot be made about the trend because of the limited number of data points.

4.3.3. Aluminum

Aluminum is an important inorganic compound produced as a result of AMD. At low pH values, the leaching of aluminum from the soil and grout may take place [25]. The U.S. EPA Water Quality Criteria limit for aluminum in natural aquatic waters is 0.75 mg/L. Time-dependent changes in aluminum concentra-

tions of leachate collected from each column are presented in Fig. 9. The concentrations stay within a narrow range for most of the columns. Some columns with relatively higher lime activator contents (F2, F3, and F4) exhibit an initial increase in
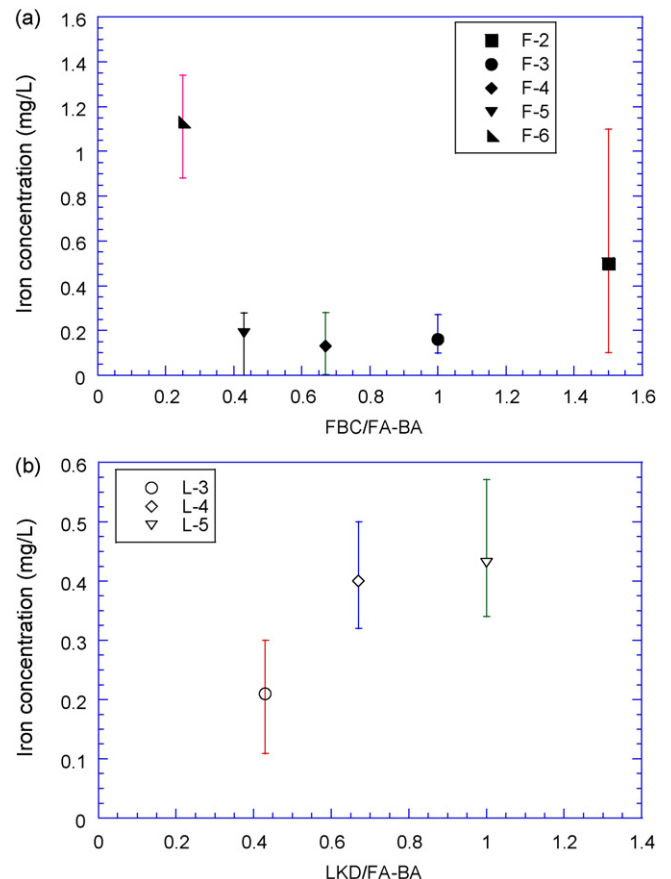

Fig. 10. Concentration of iron in the effluent vs. (a) FBC/FA–BA and (b) LKD/FA–BA.
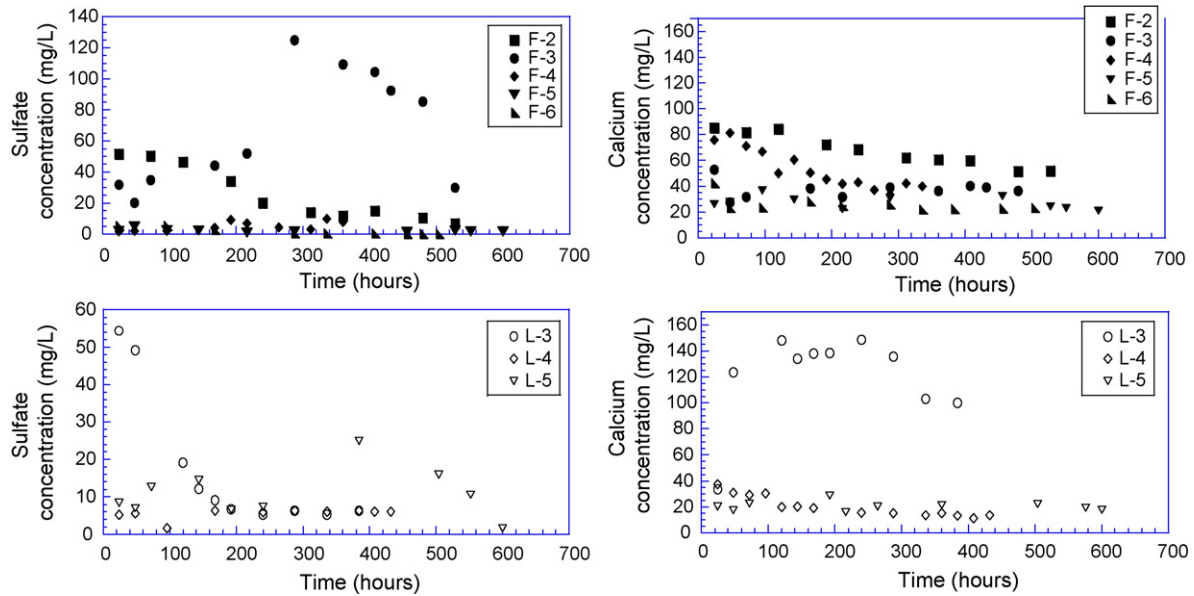
Fig. 11. Concentration of calcium and sulfate in the effluent vs. time for FBC-based, and LKD-based grout mixtures.

their aluminum concentrations, most probably due to the presence of considerable amounts of aluminum in the FBC (15.1%). All columns except F2 and F4 have final aluminum concentrations lower than the U.S. EPA limit of 0.75 mg/L. However, the values decrease after a period of time, which indicates that the concentrations are likely to further decrease in the long-term.

4.3.4. Sulfate

Analyses of sulfate concentrations in the leachate are essential since high sulfate amounts indicate the production of alkalinity due to reactions of CaO in the grout with carbon dioxide and water (Eqs. (1) and (2)). The sulfate concentrations stay in a wide range (0.1–125 mg/L) and relatively high concentrations of sulfate observed in the leachate (see Fig. 11) may be due to dissolution of grout and neutralization reactions (Eqs. (7) and (8)). In general, the sulfate concentrations either decreased with time or showed an initial increase followed by a gradual decrease.

For the column with the highest FBC content (F2 with 60% FBC), the initial concentration of sulfate in the leachate is high (51.5 mg/L), and the concentration decreases to a value of 7 mg/L in 528 h. A similar decrease from 54.3 to 6.2 mg/L in 384 h can be observed for column L3, which was the column with the highest LKD content. The initially observed high concentrations in these two columns may have been due to the dissolution of the high lime content grout. However, due to rapid hardening, the grouts may have dissolved at a much lower rate after some time, as indicated by a rapid decrease in their sulfate concentrations.

Conversely, the sulfate concentration of column F3 is initially lower than that for F2. The delayed hardening of this grout allowed for continuing dissolution. This can be observed from Fig. 11 that the sulfate concentrations gradually increase, which indicates that dissolution is still taking place. The sul-

fate reaches a peak of 125 mg/L and then gradually decreases as the grout gains strength and dissolution decreases. L5 (30% LKD) exhibits a similar trend but at a lower concentration range (1.63–25 mg/L and then down to 1 mg/L) due to the presence of relatively lower free lime content. These findings are consistent with the observations made by Laperche and Traina [27]. During remediation of AMD from Roberts–Dawson mine in Ohio, they reported a similar trend, a peak and a subsequent decrease in sulfate concentration with flue gas desulfurization grout.

The relatively low FBC content of F4 (40%) results in much lower sulfate concentrations as compared to F2 and F3 (Fig. 11). Columns F5 and F6 (FBC contents of 30% and 20%, respectively) also showed very low sulfate concentrations, with concentrations reaching almost zero with time. These low concentrations may have been due to the depletion of the little amount of free lime present in the grout.

4.3.5. Calcium

Calcium concentrations in the leachate define the degree of dissolution of grout (Eqs. (1) and (2)) and neutralization of acidity (Eqs. (7) and (8)). Therefore, analyses of calcium concentrations in the leachate are important to predict the efficiency of the grout in producing alkalinity and to determine its potential to remediate AMD. Fig. 11 shows the changes in concentrations of calcium for different pyrite-grout columns with time. In general, the calcium concentrations show a decreasing trend with time. The decrease in calcium concentrations may be attributed to hardening of the grout, which caused the grout to dissolve at a slower rate. In general, the decrease was more rapid for grout mixtures with higher lime content due to the rapid hardening of these grouts.

The initial calcium concentrations for each grout mixture generally corresponded to the amount of free lime available in the mixture. For example, for the grout mixture with highest
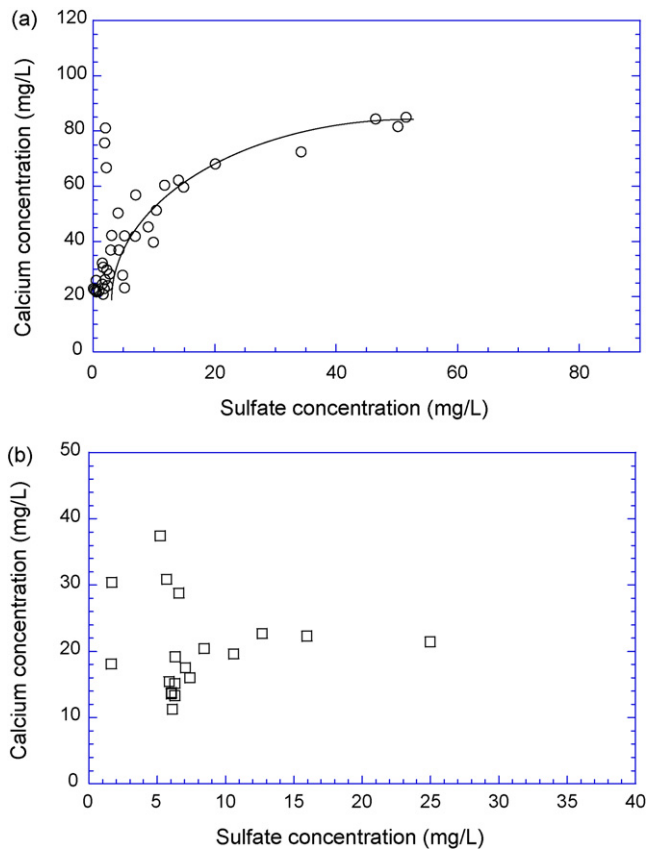
Fig. 12. Concentrations of calcium vs. concentrations of sulfate in the effluent for (a) FBC-based and (b) LKD-based grout mixtures.

FBC content (F2 with 60% FBC) the initial calcium concentration was approximately 72 mg/L, and for the mixture with lowest FBC content (F6 with 20% FBC) the initial concentration was approximately 40 mg/L, which immediately dropped to about 23 mg/L. This indicates that the calcium concentrations in the leachate are in fact due to the dissolution of grout and neutralization reactions.

The concentrations of calcium in the leachate are plotted against the concentrations of sulfate for FBC and LKD-based columns in Fig. 12. The calcium concentrations increase with increasing sulfate concentrations, which indicates that the neutralization reactions are taking place and sufficient FBC is present to neutralize acidity. Calcium concentrations tend to increase initially with increasing sulfate concentrations for LKD-based columns; however, no clear trend can be observed due to scatter in data.

5. Summary and conclusions

A study was conducted to investigate the effectiveness of an integrated technology to remediate AMD from abandoned mines through encapsulation of pyrite using CCBs and neutralization of the acidic leachate. Grouts prepared with various ratios of CCBs, and LKD were tested for geomechanical properties including spread, slump, bleed, and strength. Eight "optimal" grout mixtures were selected and evaluated for their ability to encapsulate pyrite and neutralize AMD in column tests. Hydraulic conductivity of pyrite-grout columns was measured and the leachate collected from the columns was tested for various AMD-related parameters including pH, and the concentrations of iron, aluminum, calcium, and sulfate. The following conclusions are advanced from the current work:

1. Laboratory geomechanical testing of grout mixtures using FA–BA, and FBC or LKD indicated that all materials are highly sensitive to the initial water contents and a slight variation in water content has a considerable effect on the flow (spread) of the grout. The mechanical properties of the grout such as spread, slump, bleed, and the strength were dependent on the FA–BA mix and free lime contents. In general, an increase in free lime content/FA–BA ratio increased the strength and decreased the spread, slump, and bleed of the grout.
2. Hydraulic conductivities of pyrite-grout columns ranged from 5.3×10^{-5} to 2×10^{-2} and from 2.4×10^{-5} to 1.5×10^{-2} cm/s for the FBC-based and LKD-based pyrite grout mixtures, respectively, and were relatively higher than expected. This phenomenon was attributed to the coating of the pyrite rock with the grout rather than the filling of all of the void spaces, even though the volume of grout used was nearly equal to the volume of voids present in the pyrite. Therefore, the columns represented the pyrite rock present on the mine pavement and walls of the mine shaft that has been "properly" encapsulated by grout.
3. The pH of leachate ranged from 7.6 to 8.5 for the FBC-based columns and from 8.8 to 12.3 for LKD-based columns, and generally increased with increase in the free lime content of the grout. The iron and aluminum concentrations followed a decreasing trend with time. The rate of decrease of iron was slower for grouts with relatively higher free lime contents, due to rapid hardening and the low dissolution rates of the grouts. The sulfate concentrations were highly dependent on the free lime content of the grout mixtures. The steady increase of sulfate with the addition of free lime (CaO) indicated that neutralization reactions were occurring during encapsulation process.
4. The leaching tests indicated that the presence of high amounts of lime in a grout was not solely sufficient to improve the quality of AMD, since the rate of dissolution of a high lime content grout may be slow due to its rapid hardening. Conversely, low amounts of free lime may not provide sufficient strength to the grout to efficiently encapsulate pyrite and deplete quickly, thus not providing alkalinity to the AMD in the long-run. Therefore, it is recommended that the grouts be selected considering their hardening capacities (e.g., strength) as well as the percentage of lime content present in the mixture. Based on the CCBs and pyrite used in the current study, lime contents of 40–50% can produce grouts with satisfactory geomechanical properties and acceptable levels of metal leaching; however, the data are specific to the materials employed in the current study and laboratory tests should be conducted before CCB-based encapsulation of pyrite in the field.

References

[1] P.E. Zurbuch, Neutralization of acidified streams in West Virginia, Fisheries 9 (1984) 42–47.

[2] J. Skousen, P. Ziemkiewicz, Acid Mine Drainage Control and Treatment, 2nd ed., National Mine Land Reclamation Center, Morgantown, West Virginia, 1996.

[3] P.E. Zurbuch, Early results from calcium carbonate neutralization of two West Virginia rivers acidified by mine drainage, Proceedings of the 17th West Virginia Surface Mine Drainage Task Force Symposium, Morgantown, WV, 1996, pp. L1–L9.

[4] F.T. Caruccio, G. Geidel, R. Williams, Induced alkaline recharge zones to mitigate acid seeps, Proceedings of the National Symposium on Surface Mining, Hydrology, Sedimentology and Reclamation, University of Kentucky, Lexington, KY, 1984, pp. 43–47.

[5] D. Turner, D. McCoy, Anoxic alkaline drain treatment system a low cost acid mine drainage treatment alternative, Proceedings of the 1990 National Symposium on Mining, Lexington, KY, 1990.

[6] R.S. Hedin, G.R. Watzlaf, R.W. Nairn, Passive treatment of acid mine drainage with limestone, J. Environ. Qual. 23 (1994) 1338–1345.

[7] P.F. Ziemkiewicz, J.G. Skousen, R. Lovett, Open limestone channels for treating acid mine drainage: a new look at an old idea, Green Lands 24 (1994) 36–41.

[8] P.F. Ziemkiewicz, J.G. Skousen, D.L. Brant, P.L. Sterner, R. Lovett, Acid mine drainage treatment with armored limestone in open limestone channels, J. Environ. Qual. 26 (1997) 1017–1102.

[9] P.G. Whitehead, B.J. Cosby, H. Prior, The Wheal Jane wetlands model for bioremediation of acid mine drainage, Sci. Total Environ. 33 (2005) 125–135.

[10] P.G. Whitehead, G. Hall, C. Neal, H. Prior, Chemical behavior of the Wheal Jane bioremediation system, Sci. Total Environ. 338 (2005) 41–51.

[11] C.A. Cravotta, Size and performance of anoxic limestone drains to neutralize acidic mine drainage, J. Environ. Qual. 32 (2003) 1277–1289.

[12] D.B. Johnson, K.B. Hallberg, Acid mine drainage remediation options: a review, Sci. Total Environ. 338 (2005) 3–14.

[13] K.L. Harshberger, J.J. Bowders, Acid mine drainage control utilizing fly ash, Proceedings of the ASCE Energy Division Specialty Conference on Energy in the 90's, 1991, pp. 300–1305.

[14] D.D. Gray, T.P. Reddy, D.C. Black, P.F. Ziemkiewicz, Filling abandoned mines with fluidized bed combustion ash grout, in: A.K., Howard, J.L., Hitch (Eds.), Design and Application of Controlled Low-Strength Materials (Flowable Fill), ASTM STP 1331, Philadelphia, PA, 1998, pp. 180–193.

[15] H.J. Siriwardane, R.S.S. Kannan, P.F. Ziemkiewicz, Use of waste materials for control of acid mine drainage and subsidence, J. Environ. Eng. 129 (2003) 910–915.

[16] P. Taerakul, M. Lamminen, Y. He, H. Walker, S.J. Triana, E. Whitlatch, Long-term behavior of fixated flue gas desulfurization material grout in mine drainage environments, J. Environ. Eng. 130 (2004) 816–823.

[17] M.A. Gabr, E. Boury, C. Butler, Fly ash-based mixtures for low permeability grouts, Geotech. News 14 (1996) 26–30.

[18] S. Bulusu, A.H. Aydilek, P. Petzrick, R. Guynn, Remediation of abandoned mines using coal combustion by-products, J. Geotech. Geoenviron. Eng. 131 (2005) 958–969.

[19] F.F. Ferraris, C. Lobo, Processing of HBC, Concrete International 20, 1998, pp. 61–64.

[20] P. Petzrick, Maryland Department of Natural Resources, Annapolis, Maryland, Personal communication, 2004.

[21] A. Tuncan, M. Tuncan, H. Koyuncu, Use of petroleum contaminated drilling wastes as subbase material for road construction, Waste Manage. Res. 18 (2000) 489–505.

[22] T. Lee, J. Park, J. Lee, Waste green sands as reactive media for the removal of zinc from water, Chemosphere 56 (2004) 571–581.

[23] J. Mirza, M.S. Mirza, V. Roy, K. Saleh, Basic rheological and mechanical properties of high-volume fly ash grouts, Construct. Build. Mater. 16 (2002) 353–363.

[24] U.S. EPA., National recommended water quality criteria, online document (http://www.epa.gov/waterscience/criteria/nrwqc-2004.pdf), 2004.

[25] J. Schueck, J. Tarantino, T. Kania, B. Scheetz, The use of FBC ash for alkaline addition at surface coal mines, in: Proceedings of the International Ash Utilization Symposium, Lexington, Ky., 2001. Paper No. 49.

[26] P.C. Singer, W. Stumm, Acid mine drainage: rate-determining step, Science 167 (1970) 1121–1123.

[27] V. Laperche, S.J. Traina, Flue gas desulfurization by-product weathering by acidic mine drainage, J. Environ. Qual. 28 (1999) 1733–1741.